Wireless Powered Capsule Robots With a Wide Locomotion Range and Random Orientation via Planar Transmitting Coils

Tianxiang Zheng , Ning Kang , Christopher H. T. Lee , *Senior Member, IEEE*, and Lei Shao , *Member, IEEE*

Abstract—Capsule endoscopy and drug delivery hold great promise but are constrained by power supply limitations. This study introduces a battery-free capsule robot powered by wireless power transfer (WPT), utilizing a phase-controlled 2D planar array operating at 6.78 MHz. This setup provides a stable energy supply for a micro capsule robot in a dynamic 3D space. The robot's receiving coils and on-board circuits are optimized to consistently acquire approximately 1 W of power across various positions and orientations. This enhancement significantly boosts the robot's capabilities, including high-resolution imaging and extended wireless communication. We demonstrate that the capsule can capture and transmit high-resolution images via Wi-Fi, and successfully operated in an ex-vivo digestive system, supporting its potential for biomedical applications within the gastrointestinal tract. This research also advances the WPT technology, paving the way for its use in other miniature biomedical devices and expanding their practical applications.

Index Terms—Wireless power transfer (WPT), capsule robot, magnetic field shaping, miniature medical robots, dynamic energy regulation.

I. INTRODUCTION

IN RECENT years, the healthcare industry has witnessed significant advancements in the development of minimally invasive and miniaturized biomedical devices [1], [2], [3], [4], [5]. Among these, capsule endoscopy is known for its revolutionary gastrointestinal diagnostic and therapeutic potential [6], [7], [8]. These small, autonomous devices can travel through human digestive tracts, providing valuable endoscopic information through real-time videography and sensing. For instance, Saransh et al. developed a three-dimensional localization method for capsules using on-board Hall magnetic field sensors to determine the strength of the magnetic field in a constructed 3D linear-gradient external field, thus enabling three-dimensional positioning [9]. Hou et al. developed a swallowable

X-ray dosimeter capable of real-time monitoring of radiation, pH, and temperature in the gastrointestinal tract, enhancing the precision of radiotherapy for gastrointestinal cancer [10]. Srinivasan et al. developed a vibrating ingestible bioelectronic stimulator pill which introduces a novel ingestible device that modulates gastric stretch receptors through luminal vibratory stimulation, inducing illusory satiety and reducing food intake and weight gain [11]. Inda-Webb et al. demonstrated a sub-1.4 cm^3 ingestible capsule that integrates genetically engineered probiotic biosensors with low-power electronic circuits for wireless detection of labile inflammatory biomarkers in the gastrointestinal tract, enabling earlier diagnosis and accurate tracking of inflammatory bowel disease. [12]. Gao et al. developed an ingestible microneedle capsule robot inspired by the porcupinefish that uses intestinal peristalsis to inject drugs directly into the intestinal wall, showing promise for pain-free oral drug delivery with efficacy comparable to subcutaneous injections [13].

In spite of their accomplishment, existing capsule robots rely on small coil cell batteries as power sources, which not only severely limits their operational period but also reduces the possibility of including energy-hungry applications such as high-resolution imaging, multiple sensor monitoring and therapeutic functions [14], [15]. The need for a reliable and continuous energy supply in such implantable and swallowable medical devices is actually a general requirement, as it directly affects their ability to perform complex and prolonged medical tasks. In response to these challenges, there is a growing focus on exploring alternative energy solutions that can extend the operational lifetime [16], [17].

WPT technology, consisting of a transmitting coil (Tx coil) and a slightly distanced receiving coil (Rx coil) coupled via sinusoidal electromagnetic fields, represents a promising solution that offers the possibility of a continuous, wireless energy supply without the physical constraints of batteries [18]. WPT is already commercially available for energy transfer in various devices such as smartphones, watches and drones [19], [20]. These devices are typically large in size, allowing them to receive energy through WPT under relatively undemanding system parameters. However, when WPT technology is applied to small scale medical devices in which the Rx coil is drastically reduced in size and distanced by biological tissues, especially like capsules and stents, it is significantly more challenging to achieve efficient and stable transfer and thus has not been widely explored.

Among the few related works, Zhang et al. developed a wireless powered deformable stent which achieved non-invasive
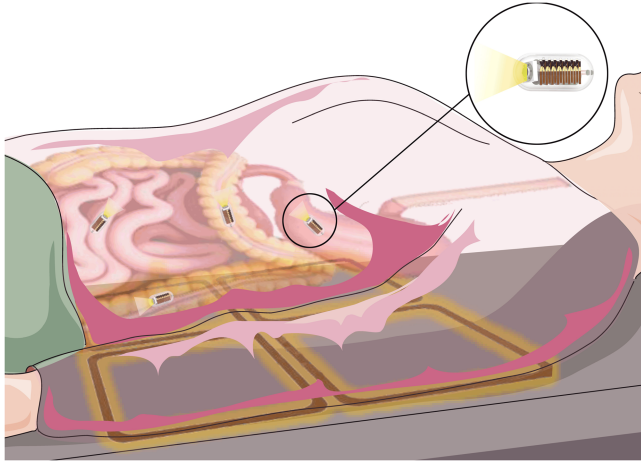
Fig. 1. The WPCR system is designed to perform medical image acquisition inside a patient's gastrointestinal system without tether and battery. The transmitter coil arrays are located outside the patient's body, with the aim of providing a constant and efficient energy supply to the capsule regardless of its position and orientation.
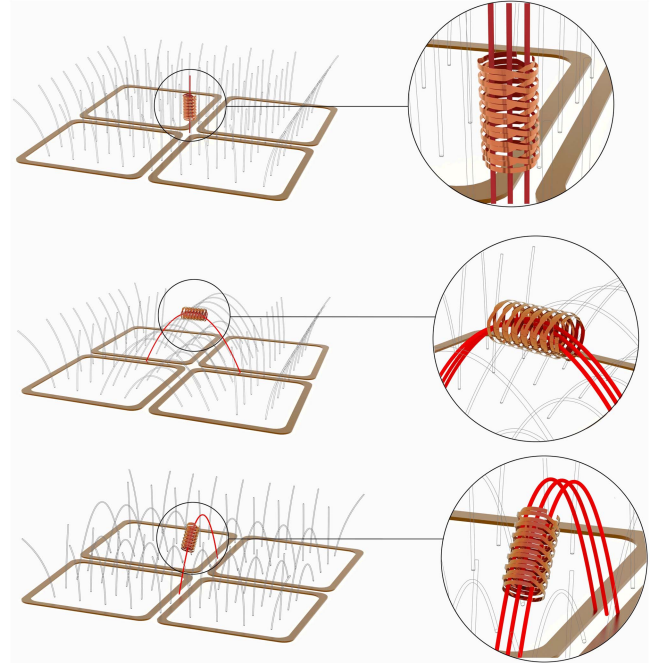

Fig. 2. Concept of magnetic field reshaping generated by the 2D planar Tx coils for stable and efficient power transfer for three different kinds of position and orientation.

electrical stimulation of the lower esophageal sphincter [21]. Kwon et al. developed a wireless implantable sensor for real-time, continuous monitoring of blood pressure, flow rate, and temperature, potentially enhancing perioperative management of cardiovascular diseases with less invasive procedures [22]. Bayvot, et al. demonstrated a multi-joint shape morphing actuator, utilizing WPT at different frequencies to selectively actuate each subdomains of the actuator by electromagnetic resonance [23]. The above biomedical devices powered WPT are still limited to their specific physiological regions with little change in position and orientation, which is due to the necessity of carefully aligned coupling electromagnetic fields to maintain a stable power transmission. This is distinctively different and simplified comparing to the situation of a capsule inside human body. Most recently, there is a single study by Gao et al. which addressed the energy supply issue of a capsule robot with random orientations by a rotational 2D Tx coil (effective 3D) but the position of the capsule is yet still fixed at the center of the Tx coil [24].

Overall, there is no study so far reporting a capsule robot powered by WPT and at the same time featuring widely changing position and orientation as if travelling through human body. Here, we propose a wireless powered capsule robot (WPCR) that could receive a stable power of approximately 1 W regardless of its position and orientation as long as it is maintained a certain distance from Tx coil. This system employs a 2D planar Tx coil array with feedback controlled real-time 3D shaping of the magnetic field so that the flux is always aligned well with the Rx coil inside the capsule robot. As a result, the capsule robot could receive a continuous and stable energy supply when moving passively through human gastrointestinal systems, as the patient lies prone or supine on the planar Tx coils. (as shown in Fig. 1) Such a 2D Tx coil provides an alternative method over robotic tracking systems [25], leading to no moving parts and easier integration in beds or wearable vests. In addition, the size of the Rx coil is miniaturized by drastically reducing the number of coil turns due to the selection of a high WPT frequency at 6.78 MHz. The capsule robot is also equipped with on-board

voltage regulation circuits, cameras, data processing and Wi-Fi communication modules. We finally show the recorded power of the WPCR at various positions and orientations, and high-resolution images captured and sent in real time. Such a WPCR could pave the way for future battery-less capsule robot for high-performance videography, drug delivery, electrical stimulation, and thermal ablation therapy [26], [27].

II. CONCEPT OF WIRELESS POWERED CAPSULE ROBOTS

The primary challenges in reliably powering a capsule robot via WPT are its wide range of positions and random orientations, coupled with the small size of the Rx coil. Most existing WPT systems necessitate that the receiving device remains static to align with the Tx magnetic flux.

In order to expand the position range of the receiving device and given the deployment goal inside human gastrointestinal systems, a 2D planar Tx coil is selected as building blocks to form an array so that it could be selectively powered to cover the wide possible range of the capsule robot. More important, because the capsule robots travel through human bodies passively with unpredictable, changing orientations, it would be important to reshape the magnetic flux so that it automatically aligns with the Rx coil. To achieve such a purpose, the position and orientation of the Rx coil are detected by changes in the mutual inductance between the Rx coil and each transmitting unit in the Tx array, followed by a synergistic phase control among each transmitting unit in the planar array to re-shape the 3D magnetic field, which can be tailored to suit the receiver device at different spatial locations and energy demands, as in Fig. 2. Furthermore, the planar Tx array greatly improves convenience and provides the possibility of a flexible or wearable Tx array in the future [28], [29].
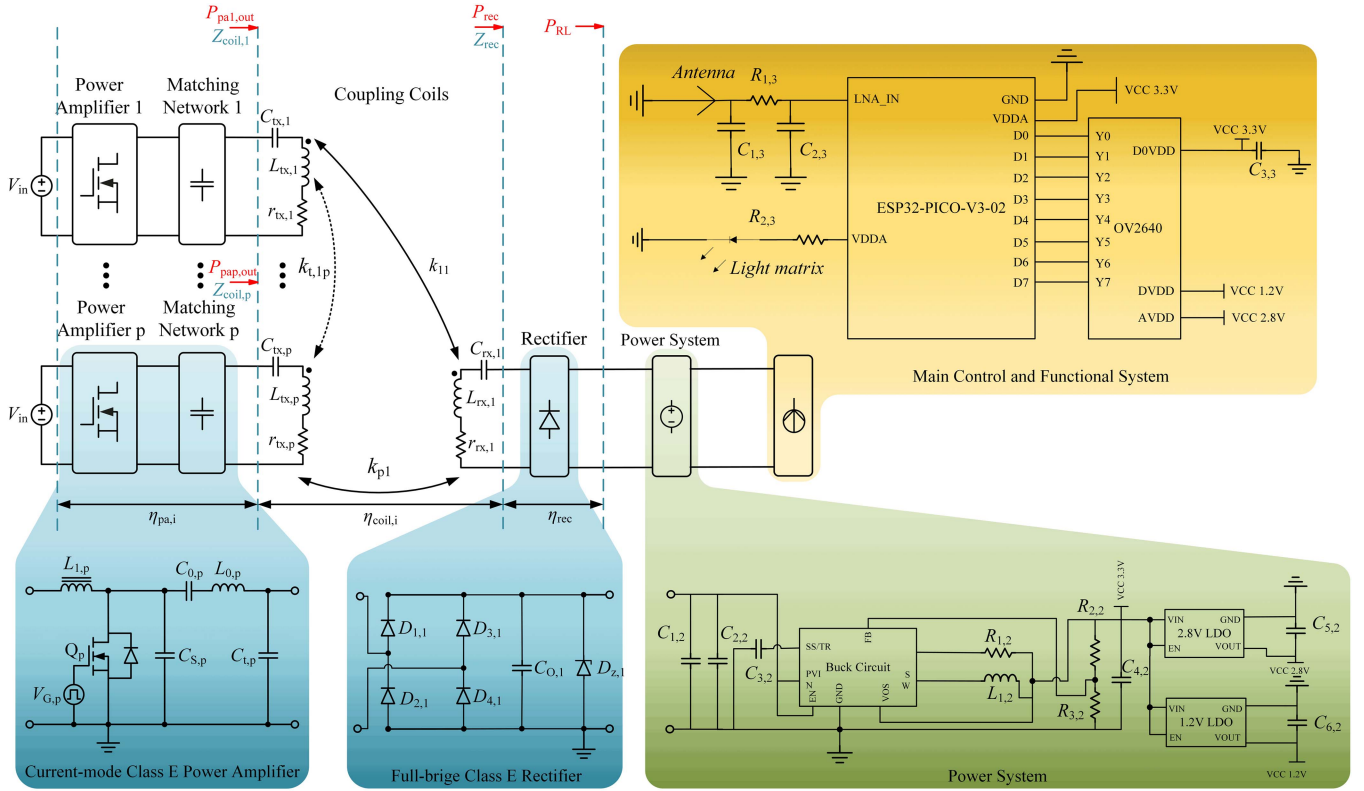
Fig. 3. Overall design of the WPCR system. The blue panel shows the wireless power Tx coil array and the Rx coil. The green panel shows the power conversion module inside the capsule robot, followed by a yellow panel showing the control and functional module inside capsule robot.

Fig. 2 shows three representative kinds of position and orientation of the capsule robot, with adjusted 3D magnetic flux shaping. The first condition shows that the Rx coil is positioned vertically on top of the transmitting array, and thus the transmitting units are driven all at the same phase so that the magnetic flux is also along the vertical direction and perfectly aligns with the Rx coil. The second condition shows a horizontally positioned capsule robot, where the two transmitting units are driven in opposite phase to the units on the right side, yielding a horizonal flux at the Rx coil. The last condition adjusts the magnetic flux according to the same spirit to yield highly aligned flux along the Rx coil. Such a real-time magnetic flux reshaping scheme could guarantee a stable and efficient power transfer to a capsule robot. Sophisticated electrical and control design are required to achieve this scheme and are detailed in following sections.

III. DESIGN OF WIRELESS POWERED CAPSULE ROBOTS

The architecture of the proposed WPCR consists of three main modules, distinguished by different colors in Fig. 3: the wireless power transmitting and receiving module (blue), the power conversion module (green), and the main control and functional module (yellow).

A. Wireless Power Transmitting and Receiving Module

This module is consisting of the transmitting component and the receiving component, where the former is located outside of human body and the latter is located inside the capsule robot (as shown in the blue panel in Fig. 3). The transmitter is built

as a scalable planar coil array based on a resonant frequency of 6.78 MHz to provide energy to a single target receiver. This design utilizes multiple current-mode Class E power amplifiers (PAs) in parallel, enabling them to drive individual Tx coil separately or in concert to cater for capsule robots with varying spatial locations and power requirements. The design of these PAs is optimized for radio frequency (RF) energy transfer efficiency and stability, with the objective of minimizing energy loss.

In the design of each Class E PA, a T-matching network is introduced to match the impedance between the power amplifier and the Tx coil. The T-matching network simplifies the configuration by adding a parallel capacitor $C_{t,p}$ to the physical design. The capacitor, in conjunction with the output inductance of a conventional Class E PA and the self-inductance of the Tx coil, reduces the number of components in the network, thus simplifying the design and tuning process of the entire system.

On the receiver side, the design comprises a Rx coil and a full-bridge Class E rectifier. The rectifier employs advanced rectifier bridge chip technology on a flexible circuit board, which ensures excellent power conversion and adaptability to load variations of the camera and Wi-Fi. The use of rectifier bridge chips also helps to reduce the module size, providing for optimization of the internal space inside the miniaturized capsule robot.

B. Power Conversion Module

The power processing and conversion module (as shown in the green panel in Fig. 3) comprises a synchronous buck converter and two low dropout regulators (LDOs). The main function of the LDO is to convert the RF energy collected by the receiver coil

into a stable DC voltage, which is designed to be 3.3 V. Through efficient power conversion, the buck converter ensures a stable power output for the main control system of the capsule robot, even under different loading conditions. The buck converter provides a reliable power base for the main control system of the capsule robot. The two LDOs are responsible for providing two additional different DC voltage outputs (2.8 V and 1.2 V) to feed different on-board functional modules. The outputs of these regulators are further stabilized by a series of decoupling and filtering capacitors in order to ensure the purity and stability of the power supply and to avoid high-frequency switching noise which could interfere the capsule robot's internal precision electronics.

C. Main Control and Functional Module

The core of the main control and functional module (as shown in the yellow panel in Fig. 3) is a microcontroller chip (MCU, ESP32-PICO-V3-02), which has a rich feature set and a large-capacity memory. This enables the MCU chip to process and store high-resolution video and image data. The ESP32 chip is equipped with an 8 MB SPI Flash and a 2 MB SPI PSRAM, enabling it to process complex data streams in real time and cache large amounts of information for analysis. The chip's high-speed Wi-Fi communication function supports rapid and stable image data transmission, even in dynamic in-vivo environments, because Wi-Fi features higher bandwidth, longer range, and established infrastructure in healthcare settings, ensuring reliable real-time image transmission and secure data transfer with WPA3 encryption [30].

The on-board camera (OV2640) provides the system with the capacity to capture high-resolution images. This is achieved by means of a direct connection with the MCU chip, facilitated by the presence of eight I/O ports. At the same time, this camera requires three different DC voltage, and thus the precise regulation of three power supply voltages (3.3 V, 2.8 V, 1.2 V) by the power conversion module is essential to guarantee the stability of the camera operation.

To enable the illumination for the capsule robot, an LED array is designed as the main light source, ensuring the capture of clear images inside dark human gastrointestinal systems where other lighting sources are not possible. The LED array has been designed around the camera, with due consideration of internal space constraints and illumination requirements. Its purpose is to provide uniform and effective illumination without unduly increasing power consumption or generating excessive heat.

IV. FABRICATION OF WIRELESS POWERED CAPSULE ROBOTS

A. Parametric Design the WPT System

In this study, a 2×2 array of Tx is employed, including four planar coils and current-mode Class E power amplifiers. The receiving side comprises a Rx coil and Class E full-bridge rectifiers. By controlling the phase difference between multiple drive signals, the four Tx coils will receive currents in different phases. The four Tx coils are assembled by means of a specially designed stack, in order to compensate for the cross coupling among the Tx coils [31].

The input impedance of the class E full-bridge rectifier, Z_{rec}, can be represented as

$$Z_{\text{rec}} = R_{\text{rec}} + j X_{\text{rec}} \tag{1}$$

where R_{rec} is the resistance and X_{rec} is the reactance. To offset the reactance inherent to the rectifier, the optimal capacitance of the Rx coil must fulfill the following relationship as

$$j\omega L_{\text{rx}} + \frac{1}{j\omega C_{\text{rx}}} + j\ X_{\text{rec}} = 0 \tag{2}$$

where L_{rx} is the inductance of the Rx coil, L_{tx} is the inductance of the Tx coil, and ω is the resonance frequency of the WPT system, namely, $2\pi \cdot 6.78$ MHz here. Then the compensation capacitor of the Rx coil can be derived as

$$C_{\text{rx}} = \frac{1}{\omega\left(\omega L_{\text{rx}} + X_{\text{rec}}\right)} \tag{3}$$

$$C_{\text{tx}} = \frac{1}{\omega^2 L_{\text{tx}}} \tag{4}$$

Impedance variations resulting from alterations in the coupling coefficient (k) detune the resonance of the coupling coil and impair the performance of the power amplifier. To maintain a high mutual inductance between Tx and Rx for changing positions and orientations, an impedance compression method is employed by a stacked transmitter architecture and T-shaped matching network. For coupling coils, the power loss occurs on the parasitic resistances, i.e., r_{tx} and r_{rx}. Thus, the efficiency of a pair of Tx and Rx coil, η_{coil}, can be written as

$$\eta_{coil} = \frac{R_{rec}}{\left(1 + \frac{r_{tx}r_{rx} + r_{tx}R_{rec}}{\omega^2 k^2 L_{tx} L_{rx}}\right)\left(r_{rx} + R_{rec}\right)} \tag{5}$$

The efficiency of a 2×2 array of Tx coils and a Rx coil could be calculated above using (1)–(5).

The distribution of the magnetic field at each spatial point allows an indirect calculation of the received open-circuit voltage of the Rx coil at that position. This can be obtained using the Faraday's Law of Electromagnetics with respect to the area of the Rx coil S, the number of turns of the coil N, and the maximum magnetic field strength $|B|$. Therefore, the induced root mean square (RMS) of the open-circuit voltage of the Rx coil can be calculated by obtaining the magnetic field strength at the location of the Rx coil as

$$V_{oc} = \frac{\sqrt{2}}{2}\ \cdot \omega \cdot |B| \cdot N \cdot S \tag{6}$$

It can be seen in (6) that higher frequencies also help to increase the open circuit voltage of the Rx coil, further reducing the coil size [32]. This field at any particular location could be derived by adding the vector field generated by each Tx coil [25]. The η_{coil} and V_{oc} are important indicators of WPT and whether the capsule robot can operate, and they will be measured in the subsequent experiments.

B. Real-Time Phase Control of Tx

In order to achieve efficient energy reception at the Rx coil during the random motion of the capsule robots, we adopt a dynamic detection and control strategy to shape the flux by phase adjustment of the Tx coils [33], [34], as shown in Fig. 4. The phase control system of the Tx coil can be divided into three parts. First, in the initialization part, the initial PA current detection code is implemented, and the code for initial magnetic field shaping with many commonly used field shapes are entered via a controller chip. Second, in the detection part, through detecting the current of the four PAs, we determine the position
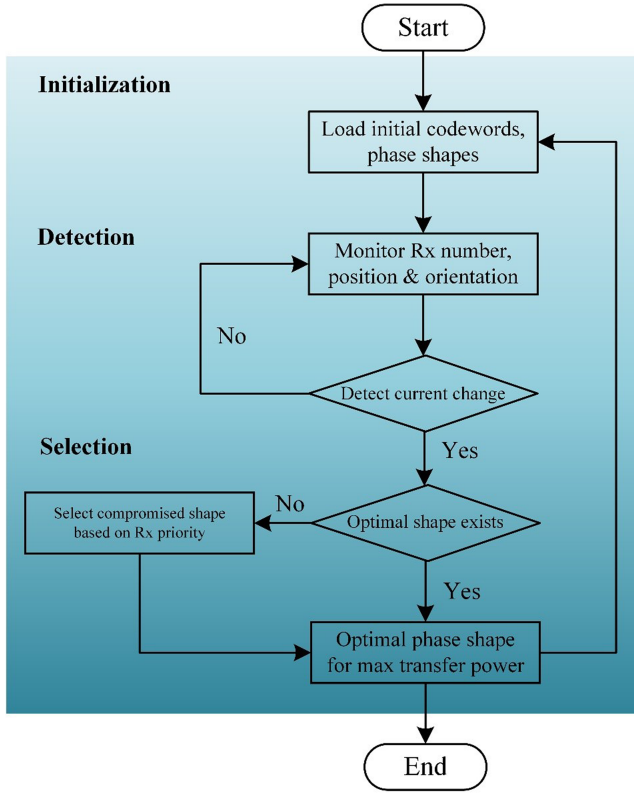
Fig. 4. Flow chart of phase control for Tx array to adjust the magnetic field for changes in position and orientation of the Rx coil inside the capsule robot.
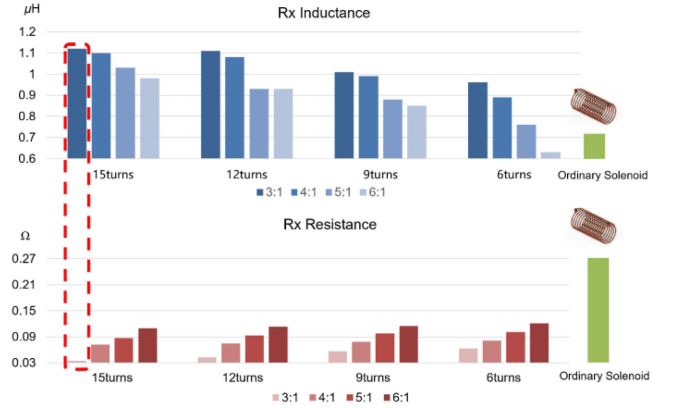

Fig. 5. The process of winding the FPCB Rx coil.

Fig. 6. Self-inductance and internal resistance of the interleaved coils with different number of turns and line width to pitch ratio.

and orientation of the Rx coil by prior known relationship between them. Third, in the selection part, through the feedback current of the four PA, we determine whether a more optimal magnetic field shape exists, and if true then we select the optimal shape for maximized transfer power. The control system runs continuously as one flux reshaping loop within 0.4 ms, and dynamically adjusts the magnetic field to ensure efficient energy transfer while recording the capsule's position and orientation.

This control system strategy is not only capable of accurately detecting the spatial positions and orientations of multiple receivers, but also of adjusting the magnetic field distribution based on this information. The control mechanism, combined with an operating frequency of 6.78 MHz, makes it possible to wireless power a miniatured Rx coil at random position and orientation consistently.

C. WPT Receiving Coils

In order to achieve efficient energy transfer to the Rx coil inside the small sized capsule, the design of the Rx coil must meet stringent dimensional and performance requirements. In this work, we choose an diameter of 1.6 cm and a length of 2.5 cm for the capsule, and thus the size of the Rx coil must be precisely controlled to fit into this space. As shown in Fig. 5, the Rx coil is made of FPCB and fits well into the capsule shell through flat folding. Although it is larger than the commercial "NaviCam", the capsule has the potential to scale down by using thinner shells and optimized receiving coil design.

In this study, a flexible printed circuit board (FPCB) based interleaved Rx coil design is used. The coils are fabricated using planar FPCBs and folded into a double-layer solenoid structure through precise winding and soldering processes. The interleaved design is intended to maximize the self-inductance of the coil and minimize its internal resistance, thereby enhancing the energy receiving efficiency. To further ascertain the optimal number of coil turns and line width to pitch ratio, a thorough simulation was conducted using the Ansys HFSS software.

The simulation, shown in Fig. 6, confirms that the interleaved FPCB Rx coil design could achieve a better performance than an ordinary solenoid design. With 15 turns, a 1 mm line width, and a 3:1 pitch ratio, it reaches the best result with a self-inductance L_{rx} of 1.12 μH and a resistance r_{rx} of 0.035 Ω. Substituting these values into (5), the transmission efficiency η_{coil} will be maximized. This interleaved structure also simplifies circuit connections by positioning the input and output ports at same ends, alleviating stringent space requirements.

D. Assembled Prototype of the Capsule Robot

As shown in Fig. 7, the circuits inside the capsule in this study includes three double-sided FPCBs with a diameter of 1.5 cm and a thickness of 0.1 mm. The front side of the system is arranged with a series of functional modules, including an LED matrix, a camera, a MCU chip, a ceramic antenna and a buck conversion circuit. The backside is equipped with rectifier bridges, matching capacitors and LDOs. It employs the double-sided feature of the FPCB to achieve a compact arrangement of electronic components, thereby making full use of the limited space to integrate all the required functions.

As the core of the energy and data processing modules, the MCU chip integrates powerful processing capability and storage capacity, which enables it to perform high-precision signal acquisition and processing. Additionally, the device incorporates
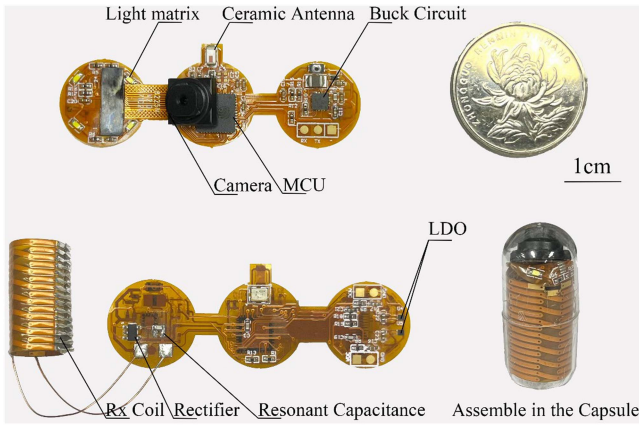
Fig. 7. Layout of the on-board circuits and the folded Rx coil.

a robust Wi-Fi functionality at a frequency of 2.4 GHz, effectively negating the potential for interference with the 6.78 MHz magnetic flux for WPT, which is proved by WPT powered videography in the next section. Furthermore, it is capable of achieving a data rate of up to 150 Mbps with a 0.4 μs protection interval. The overall device is encased in a protective epoxy resin shell with a total weight of 2.1 gram (shell: 0.9 gram; Rx coil: 0.5 gram; circuits with camera: 0.7 gram), which is only 40% of the weight of those existing commercial capsule gastroscopes [6], [7]. The most weight reduction is due to the elimination of the batteries.

V. RESULTS AND DISCUSSION

In order to better demonstrate the ability to transfer energy at various capsule positions and orientations with a useful distance, the received powers in a 20 cm × 20 cm × 20 cm cubic space above the Tx coil array are shown in Fig. 8. For each position, the capsule is oriented in a way to maximize the receiving power while the flux reshaping runs automatically. The received power gradually decreases from 1.2 W to 0.2 W, as the distance between the capsule and the Tx coil array increases. This result indicates that our system is capable of providing robust power within clinically relevant ranges, such as the gastrointestinal tract from the abdominal surface. It also provides the possibility for a supine position of the patient with further optimization.

To evaluate the effectiveness of the WPCR system in maintaining stable energy reception for the main MCU and camera under random position and orientation in biological environments, the transmittion efficiency(η_{coil}) and open-circuit voltage (V_{oc}) were precisely measured under various barrier materials at heights ranging from 1 to 6 cm. The transmission system was connected to a stable 30 V input voltage and combined with FPGA for automatic field shaping adjustment, ensuring optimal magnetic field distribution for the Rx coil. As shown in Fig. 9, the experimental results indicate that the system meets its energy requirements under various barrier conditions (V_{oc} over than 3.3 V), with the air medium leading to the highest η_{coil} and V_{oc}, and the biological tissue barrier showing reduced performance.

In addition, we tested the camera and Wi-Fi functions powered by WPT under continuously chaning positions and orientations of the capsule. As shown in Fig. 10 , we constructed an ex-vivo
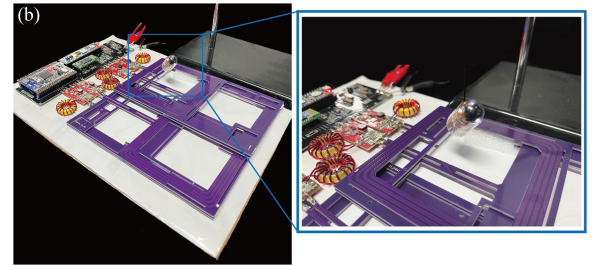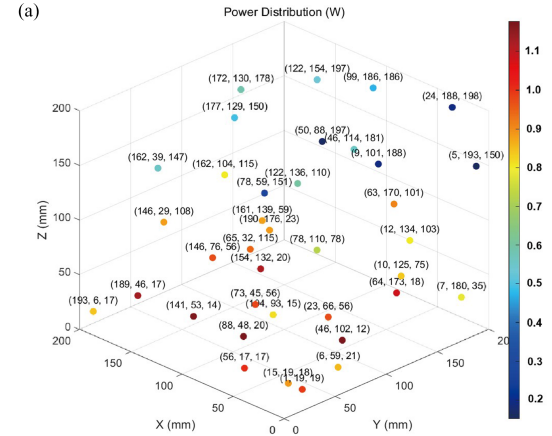
Fig. 8. (a) Received power inside a 20 cm × 20 cm × 20 cm cubic space above the Tx. (b) The WPCR suspended above the Tx coil.
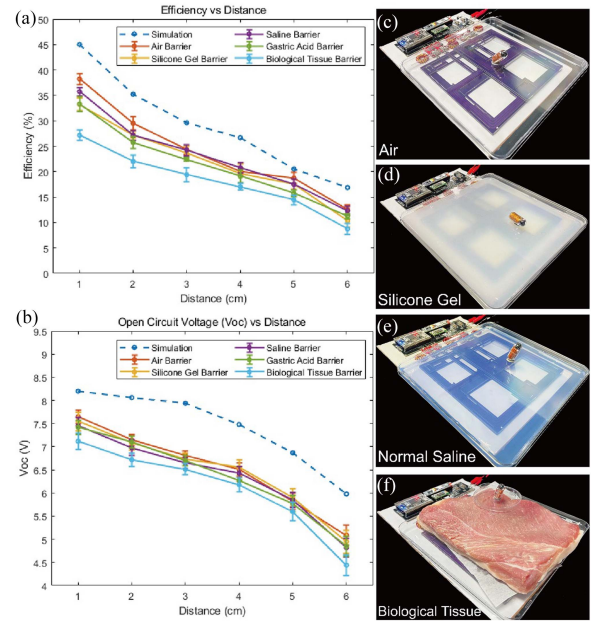
Fig. 9. (a) The efficiency (η_{coil}) and (b) The open-circuit voltage (V_{oc}) of the Rx coil over increasing distances from the Tx coil array under various barriers in between. (c)~(f) Various barrier materials between the Tx coil and the Rx coil.

experiment of a pig's gastric digestive system, where a pig's stomach and a piece of thick pork belly were layered over the Tx coil array, which creates a distance from the Tx coil of 4–5 cm. The capsule robot was pulled through the pig's stomach using a thin thread to mimic the gastrointestinal motility, while continuously transmitting captured images via Wi-Fi. Along the
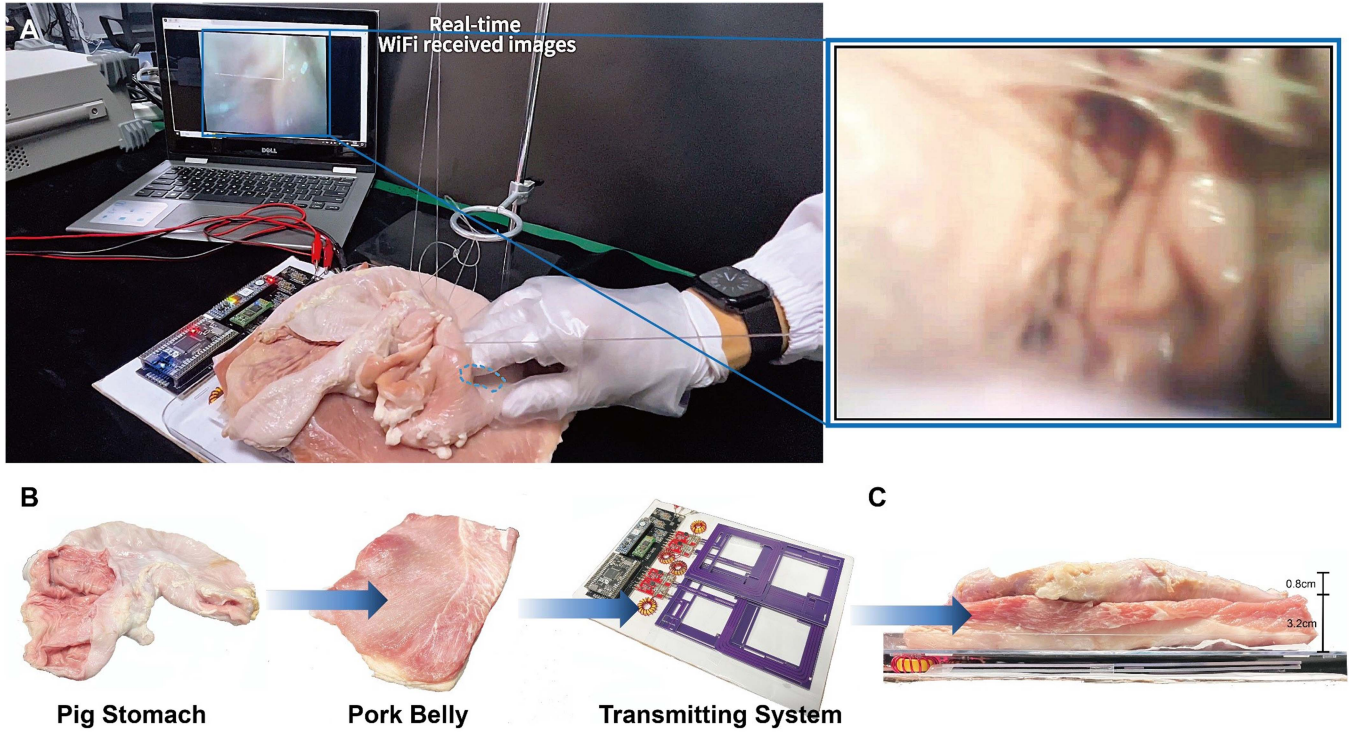
Fig. 10. (a) The WPCR moves inside a pig's stomach, while capturing and transmitting images in real-time via Wi-Fi. Video URL: WPCR Operating (https: //youtu.be/wz0ZCNSdHDg) (b) The ex-vivo setup with a pig's stomach, a piece of thick pork belly, and the transmitting system stacked together. (c) The total thickness of the barrier between the Tx and the capsule is between 4 cm and 5 cm.
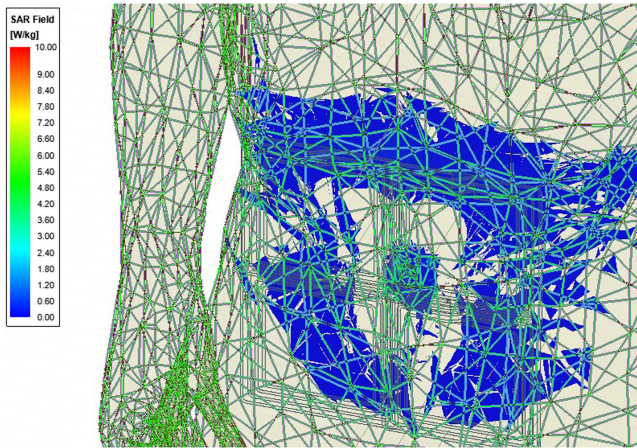

Fig. 11. The system specific absorption rate (SAR) simulated by HFSS.

trajectory, a laptop received real-time images inside the pig's stomach. These images had a resolution of 2 megapixel and a refresh rate of 15 fps. More information could be viewed in the accompanying video, which demonstrates the real-time refreshing of the images captured and transmitted by the WPCR.

To further ensure the safety of the WPT system for experimental biological subjects, we conducted a simulation analysis of the specific absorption rate (SAR) using HFSS. SAR is expressed in watts per kilogram (W/kg), representing the energy absorbed per unit mass of tissue. According to international electromagnetic safety standards, such as IEEE C95.1, SAR should not exceed 10 W/kg for the head and limbs, and 20 W/kg for the torso. SAR

could be calculated as

$$SAR = \frac{\sigma}{\rho} \cdot |E|^2 \tag{7}$$

where σ is the tissue conductivity, $|E|$ is the electric field strength, and ρ is the tissue density.

We focus on the peak SAR value with the WPCR in the digestive system to evaluate its potential impact on surrounding tissues. The peak SAR simulated by the HFSS software during operation was 0.951 W/kg (surface of the capsule robot) as shown in Fig. 11, which is well below the 20 W/kg limit for the torso, indicating that the energy absorption at this site is compliant with international safety standards.

VI. CONCLUSION

This study proposes a battery-less capsule robot with wireless power transfer of approximately 1 W of stable supply under constantly changing positions and orientations, which fully satisfies the power requirements of a camera, control, and communication chips. The known technical challenges for such a robot include dynamic locomotion, limited space, and regulated power requirements of the capsule. To address the dynamic locomotion of the capsule, we employed an FPGA-based automatic control system to dynamically reshape the magnetic field distribution emitted by a 2D planar Tx coil array, aligning the magnetic flux with the capsule's Rx coil to ensure efficient power transfer. For the limited space inside the micro capsule, we selected a high WPT frequency of 6.78 MHz and an interleaved Rx coil structure with optimized parameters, significantly reducing the number of coil turns while maintaining high inductance.

Finally, we designed double-sided multi-layer FPCB circuits to integrate on-board power regulation, control, data caching, processing, and wireless communication. Compared to the current state-of-the-art where all capsules rely on small coin cell batteries with limited operation duration and reduced image resolution and refresh rate, the capsule robot in this study demonstrates significant advantages in terms of energy-intensive metrics, such as operational duration, imaging quality, and Wi-Fi transmission range. Additionally, through power transfer across different barriers and ex-vivo experiments inside a pig stomach, the feasibility of the capsule robot in biological subjects has been validated. The application of this technology is expected to improve the quality and efficiency of gastrointestinal diagnosis, reduce patient discomfort, lower operating costs, and pave the way for potential precision therapeutic treatments.

REFERENCES

[1] A. Abramson et al., "Oral delivery of systemic monoclonal antibodies, peptides and small molecules using gastric auto-injectors," *Nat. Biotechnol.*, vol. 40, pp. 103–109, 2022.

[2] A. Canales et al., "Multifunctional fibers for simultaneous optical, electrical and chemical interrogation of neural circuits in vivo," *Nat. Biotechnol.*, vol. 33, pp. 277–284, 2015.

[3] M. A. Al-Rawhani, J. Beeley, and D. R. Cumming, "Wireless fluorescence capsule for endoscopy using single photon-based detection," *Sci. Rep.*, vol. 5, 2015, Art. no. 18591.

[4] A. Abdigazy, M. Arfan, G. Lazzi, C. Sideris, A. Abramson, and Y. Khan, "End-to-end design of ingestible electronics," *Nat. Electron.*, vol. 7, no. 2, pp. 102–118, 2024.

[5] R. Mundaca-Uribe, N. Askarinam, R. H. Fang, L. Zhang, and J. Wang, "Towards multifunctional robotic pills," *Nat. Biomed. Eng.*, no. 8, pp. 1334–1346, 2023.

[6] P. Nadeau et al., "Prolonged energy harvesting for ingestible devices," *Nat. Biomed. Eng.*, vol. 1, 2017, Art. no. 0022.

[7] K. Kalantar-Zadeh et al., "A human pilot trial of ingestible electronic capsules capable of sensing different gases in the gut," *Nat. Electron.*, vol. 1, pp. 79–87, 2018.

[8] V. Iacovacci et al., "A fully implantable device for intraperitoneal drug delivery refilled by ingestible capsules," *Sci. Robot.*, vol. 6, 2021, Art. no. eabh3328.

[9] S. Sharma et al., "Location-aware ingestible microdevices for wireless monitoring of gastrointestinal dynamics," *Nat. Electron.*, vol. 6, no. 3, pp. 242–256, 2023.

[10] B. Hou et al., "A swallowable X-ray dosimeter for the real-time monitoring of radiotherapy," *Nat. Biomed. Eng.*, vol. 7, no. 10, pp. 1242–1251, 2023.

[11] S. S. Srinivasan et al., "A vibrating ingestible bioelectronic stimulator modulates gastric stretch receptors for illusory satiety," *Sci. Adv.*, vol. 9, no. 51, 2023, Art. no. eadj3003, doi: 10.1126/sciadv.adj3003.

[12] M. E. Inda-Webb et al., "Sub-1.4 cm^3 capsule for detecting labile inflammatory biomarkers in situ," *Nature*, vol. 620, no. 7973, pp. 386–392, 2023.

[13] X. Gao, J. Li, J. Li, M. Zhang, and J. Xu, "Pain-free oral delivery of biologic drugs using intestinal peristalsis-actuated microneedle robots," *Sci. Adv.*, vol. 10, no. 1, 2024, Art. no. eadj7067.

[14] M. Mimee et al., "An ingestible bacterial-electronic system to monitor gastrointestinal health," *Science*, vol. 360, pp. 915–918, 2018.

[15] Y. Kimchy et al., "Radiographic capsule-based system for non-cathartic colorectal cancer screening," *Abdom. Radiol.*, vol. 42, pp. 1291–1297, 2017.

[16] H. Zhuang, W. Wang, and G. Yan, "Omnidirectional wireless power transfer system using modified saddle-shaped coil pair for implantable capsule robots," *IEEE Trans. Power Electron.*, vol. 38, no. 9, pp. 11664–11672, Sep. 2023.

[17] M. R. Basar, M. Y. Ahmad, J. Cho, and F. Ibrahim, "An improved wearable resonant wireless power transfer system for biomedical capsule endoscope," *IEEE Trans. Ind. Electron.*, vol. 65, no. 10, pp. 7772–7781, Oct. 2018.

[18] W. Chen et al., "A 25.6 w 13.56 MHz wireless power transfer system with a 94% efficiency GaN class-e power amplifier," in *Proc. 2012 IEEE/MTT-S Int. Microw. Symp. Dig.*, 2012, pp. 1–3.

[19] A. P. Sample, D. T. Meyer, and J. R. Smith, "Analysis, experimental results, and range adaptation of magnetically coupled resonators for wireless power transfer," *IEEE Trans. Ind. Electron.*, vol. 58, no. 2, pp. 544–554, Feb. 2011.

[20] S. Y. R. Hui, W. Zhong, and C. K. Lee, "A critical review of recent progress in mid-range wireless power transfer," *IEEE Trans. Power Electron.*, vol. 29, no. 9, pp. 4500–4511, Mar. 2013.

[21] C. Zhang et al., "Wirelessly powered deformable electronic stent for noninvasive electrical stimulation of lower esophageal sphincter," *Sci. Adv.*, vol. 9, no. 10, 2023, Art. no. eade8622.

[22] K. Kwon et al., "A battery-less wireless implant for the continuous monitoring of vascular pressure, flow rate and temperature," *Nat. Biomed. Eng.*, vol. 7, no. 10, pp. 1215–1228, 2023.

[23] M. Boyvat, J. S. Koh, and R. J. Wood, "Addressable wireless actuation for multijoint folding robots and devices," *Sci. Robot.*, vol. 2, no. 8, 2017, Art. no. eaan1544.

[24] J. Gao et al., "Stable wireless power transmission for a capsule robot with randomly changing attitude," *IEEE Trans. Power Electron.*, vol. 38, no. 2, pp. 2782–2796, Feb. 2023.

[25] G. Bandini et al., "Electromagnetic design of an inductive wireless power transfer system for endoscopic capsule," in *Proc. 2023 IEEE Int. Instrum. Meas. Technol. Conf.*, Kuala Lumpur, Malaysia, 2023, pp. 1–6.

[26] J. Keller et al., "Advances in the diagnosis and classification of gastric and intestinal motility disorders," *Nat. Rev. Gastroenterol. Hepatol.*, vol. 15, no. 5, pp. 291–308, 2018.

[27] S. S. C. Rao et al., "Evaluation of gastrointestinal transit in clinical practice: Position paper of the American and European Neurogastroenterology and Motility Societies," *Neurogastroenterol. Motil.*, vol. 23, pp. 8–23, 2011.

[28] C. Zhang, D. Lin, and S. Hui, "Basic control principles of omnidirectional wireless power transfer," *IEEE Trans. Power Electron.*, vol. 31, no. 7, pp. 5215–5227, Jul. 2016.

[29] J. Feng, Q. Li, F. C. Lee, and M. Fu, "Transmitter coils design for free-positioning omnidirectional wireless power transfer system," *IEEE Trans. Ind. Informat.*, vol. 15, no. 8, pp. 4656–4664, Aug. 2019.

[30] A. Iqbal et al., "Wireless power transfer system for deep-implanted biomedical devices," *Sci. Rep.*, vol. 12, 2022, Art. no. 13689.

[31] N. Kang, Y. Shao, M. Liu, and C. Ma, "Analysis and implementation of 3D magnetic field shaping via a 2D planar transmitting coil array," *IEEE Trans. Power Electron.*, vol. 37, no. 1, pp. 1172–1184, Jan. 2022.

[32] A. Kurs et al., "Wireless power transfer via strongly coupled magnetic resonances," *Science*, vol. 317, no. 5834, pp. 83–86, Jul. 2007.

[33] Y. Lim and J. Park, "A novel phase-control-based energy beamforming techniques in nonradiative wireless power transfer," *IEEE Trans. Power Electron.*, vol. 30, no. 11, pp. 6274–6287, Nov. 2015.

[34] Q. Zhu and P. Hu, "Field orientation based on current amplitude and phase angle control for wireless power transfer," *IEEE Trans. Ind. Electron.*, vol. 65, no. 6, pp. 4758–4770, Jun. 2017.